

## Supplementary Information

Activity trends among new molten metal catalysts for CO<sub>2</sub> and CH<sub>4</sub>  
conversion to 2:1 H<sub>2</sub>:CO syngas

Genpei Cai,<sup>a</sup> Zhiyuan Zong,<sup>a</sup> Kevin J. Smith,<sup>a</sup> D. Chester Upham<sup>\*a</sup>

<sup>a</sup> Department of Chemical and Biological Engineering, University of British Columbia,  
2360 E Mall, Vancouver, BC, Canada.

\*Corresponding author

## **Table of Contents**

- 1. Catalyst selection criteria**
- 2. Catalyst preparation**
- 3. Experimental design**
  - 3.1 Catalyst screening
  - 3.2 Stability test
- 4. Thermodynamic calculations**
- 5. Bubble column performance**
- 6. Carbon characterization**
  - 6.1 Surface reactor
  - 6.2 Bubble column reactor
- 7. References**

## 1. Catalyst selection criteria

Six criteria are used for the selection of molten metal catalyst to be screened, expanding on previous work<sup>1</sup>: (1) the metals should not form stable carbides; (2) metals must be able to be oxidized by CO<sub>2</sub> with Gibbs free energy less than 20 kJ/mol-CO<sub>2</sub> at 1000 °C; and/or (3) the formed metal oxide species must be able to be reduced by CH<sub>4</sub> with Gibbs free energy less than 20 kJ/mol-CH<sub>4</sub> at 1000 °C; (4) the metal candidate is non-toxic; (5) the melting point is less than 1000 °C or an alloy with melting point below 1000 °C with more than 15% metal is possible; and (6) the vapor pressure at 1000 °C is less than 10<sup>-4</sup> atm. In addition, nickel is tested as an alloy. These criteria result in Ni, Cu, Fe, Ge, Ag, Sn, Bi, In and Ga.

## 2. Catalyst preparation

Molten metal alloys were prepared from high purity (>99%) trace metals basis powders purchased from Sigma-Aldrich. For catalyst screening, metal powders were weighed using a digital analytic balance to obtain the desired molar compositions and were mixed thoroughly. The mixed powders were then transferred into the small crucible cup with 10mm OD\*8mm ID\*10mm height in dimension. A Lindberg/Blue M Mini-Mite™ Tube Furnace was used to melt the powder at 900 – 1050 °C with 0.24 L/min Ar and 0.05 L/min H<sub>2</sub> continuously flowing. Multiple loadings were done to get equal height on all samples. For bubble column reactor tests, indium and tin beads were prepared inside a quartz bubble column reactor at desired compositions and melted inside a MELLEN vertical tube furnace at 1016 °C with 6 sccm Ar and 3 sccm H<sub>2</sub> continuously flowing.

### 3. Experimental design

#### 3.1 Catalyst screening

The main equipment consists of gas cylinders with ultra-high purity gases (>99.9%) from Linde Canada Inc., four mass flow controllers (MFCs) from Brooks ® Instrument (SLA 5800 series), one mass spectrometer (RGA 100) from Stanford Research System, one furnace from Lindberg/Blue M, one pressure transducer (PT) and one thermocouple (TC) from Omega, and one customized surface reactor, which has the same dimensions as the one in our previous study.<sup>2</sup> The catalyst is filled into a quartz crucible cup with 10 mm OD and 8 mm ID, which is placed at the bottom of the quartz surface reactor with 14 mm OD and 12 mm ID. This reactor was chosen in order to compare catalysts based on the same surface area. This reactor system also allows for measurement of the initial rate of reaction.

A gas mixture containing 3 sccm of 2:1 CH<sub>4</sub> to CO<sub>2</sub> together with 4 sccm inert gas Argon was controlled by MFCs and sent to the surface reactor. The gases passed through the inlet tube with 1 mm ID and 10 mm OD to the surface of the molten metals, where the reaction occurred. To minimize the metal usage, crucible cups with an inner diameter of 8 mm were used for screening, so that a catalyst surface area of only 0.5 cm<sup>2</sup> was exposed to reactant gases. The product gases and the unreacted gases then passed through the 1 mm gap between the inlet tube and outer tube, and finally flowed to a mass spectrometer for analysis. The reaction temperature was set to 980 °C, which is higher than the melting point of all the metals and alloys for screening. Also, by setting to this temperature, the effect of pyrolysis is not significant, which mitigates catalyst deactivation due to carbon formation. All reactor components are made of quartz. During the first 3 minutes of catalyst screening, the flow rates were measured at room temperature (25°C) without any reactions. Then, the reactor was put inside the furnace and the catalysts experienced 3 to 4 minutes heating time to reach 980

°C. After approximately 17 to 20 minutes when the reactor was put into the furnace, the composition in outlet streams became relatively stable.

### 3.2 Stability test

The bubble column reactor was constructed similar to previous work,<sup>1</sup> and consisted of a quartz reactor tube filled with molten metal. An inner tube was inserted from the top to inject gas bubbles. The inner tube has an outer diameter (OD) of 1/8" and an inner diameter (ID) of 1 mm. The outer tube, which holds the melt, has an OD of 15 mm and an ID of 12 mm. The inner tube was immersed into the melt and positioned 0.5 cm above the bottom of the reactor. The melt had a height of 12 cm. The reactant gas mixture, consisting of 3 sccm of Ar, 2 sccm of CH<sub>4</sub>, and 1 sccm of CO<sub>2</sub>, was controlled by mass flow controllers (MFCs) and delivered to the inner tube of the bubble column reactor. As the gas mixture exited the inner tube, it immediately came into contact with the melt and rose along the bubble column reactor. The product gases and any unreacted gases exited the outer tube for analysis.

MELLEN vertical tube furnace was used to maintain a reaction temperature of 1000 °C over 22 hours. After that, the reaction temperature was increased to a maximum of 1170 °C. Both inlet and outlet streams were recorded by a mass spectrometer (UGA 100) from Stanford Research System during the reaction.

#### 4. Thermodynamic calculations

Thermodynamic calculations were performed using online FactSage<sup>3</sup> databases to find which metals satisfy the six criteria for catalyst selection. Phase diagrams were used to determine the appropriate screening temperature, 980 °C, and composition, mol%, at which all the metals and metal alloys melt – 50:50 mol%. In addition, Gibbs free energies for chemical looping reactions that metal being oxidized by CO<sub>2</sub> and metal oxide being reduced by CH<sub>4</sub> (Fig.S1), were calculated to investigate the correlation between catalyst performance and thermodynamics. Both Gibbs free energies for the metal being oxidized by CO<sub>2</sub> and the metal oxide being reduced by CH<sub>4</sub> are calculated based on one mole of CO<sub>2</sub> and one mole of CH<sub>4</sub>.

To determine the most stable oxidation form of the metal, we used the **Equilib** module in FactSage. By inputting a mixture of the metal and CO<sub>2</sub> at 980°C and 1 atm, we obtained the most stable oxide formation. For example, when inputting In and CO<sub>2</sub>, In<sub>2</sub>O<sub>3</sub> was determined to be the most stable oxide among the products. Then, in the **Reaction** module, we inputted the balanced equation:  $2/3\text{In} + \text{CO}_2 \rightarrow 2/3\text{In}_2\text{O}_3 + \text{CO}$ , and obtained the Gibbs free energy for this equation as the Gibbs free energy of metal oxidation.

For the reduction of metal oxide by CH<sub>4</sub>, we inputted the balanced equation for the most stable metal oxide being reduced by CH<sub>4</sub> to form pure metal, CO, and H<sub>2</sub> in the **Reaction** module. In the case of In<sub>2</sub>O<sub>3</sub>, the balanced equation was:  $2/3\text{In}_2\text{O}_3 + \text{CH}_4 \rightarrow \text{In} + \text{CO} + 2\text{H}_2$ .

In addition, the **Equilib** module in FactSage was used to calculate the equilibrium product composition as a function of temperature with a 2:1 CH<sub>4</sub>:CO<sub>2</sub> feed ratio. We inputted 2 moles of CH<sub>4</sub> and 1 mole of CO<sub>2</sub> at 1 atm as the feed gases, and **Equilib** calculated the most stable products for different temperatures (Fig.S2a). It can be observed that when the temperature

exceeds 950°C, H<sub>2</sub>, CO, and solid carbon are the most stable and main species in the product stream, with a 2:1 H<sub>2</sub>:CO ratio. Therefore, selecting a reaction temperature above 950°C is reasonable. Equilibrium CH<sub>4</sub> and CO<sub>2</sub> conversions were calculated using FactSage at 1 atm, 10 atm, and 20 atm, with a 2:1 CH<sub>4</sub>:CO<sub>2</sub> feed ratio. The results showed that both conversions decrease as the reaction pressure increases. Additionally, at temperatures above 950°C, both CH<sub>4</sub> and CO<sub>2</sub> conversions exceed 99%.

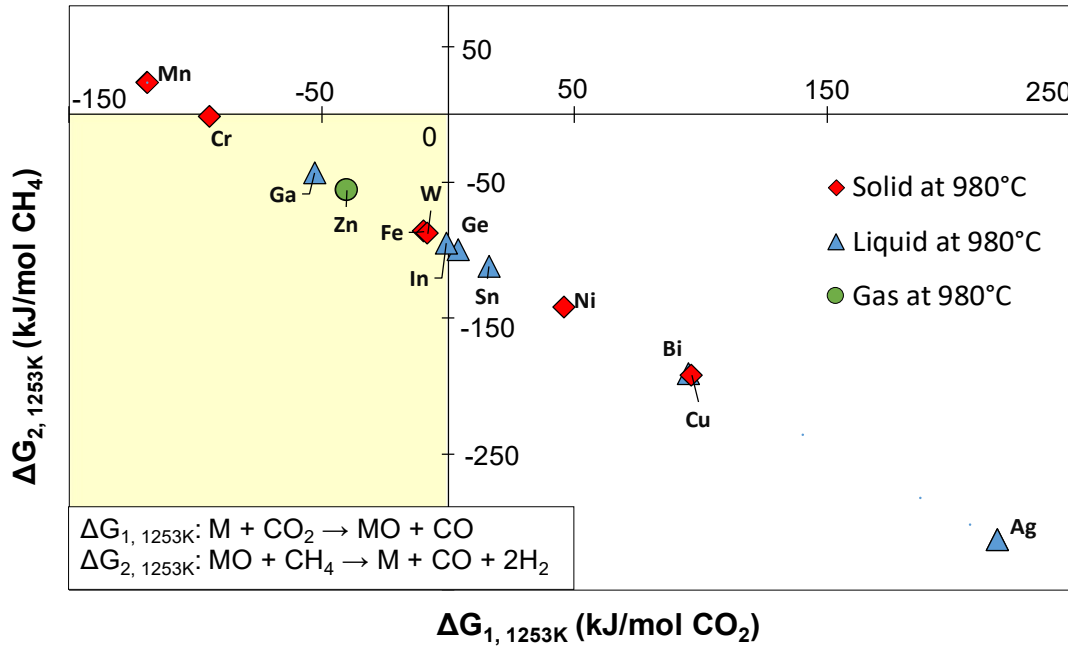


**Fig.S1** Gibbs free energy (kJ/mol) for reaction 1, metal been oxidized by CO<sub>2</sub>; and reaction 2, metal oxides been reduced by CH<sub>4</sub> at 980°C (1253K).

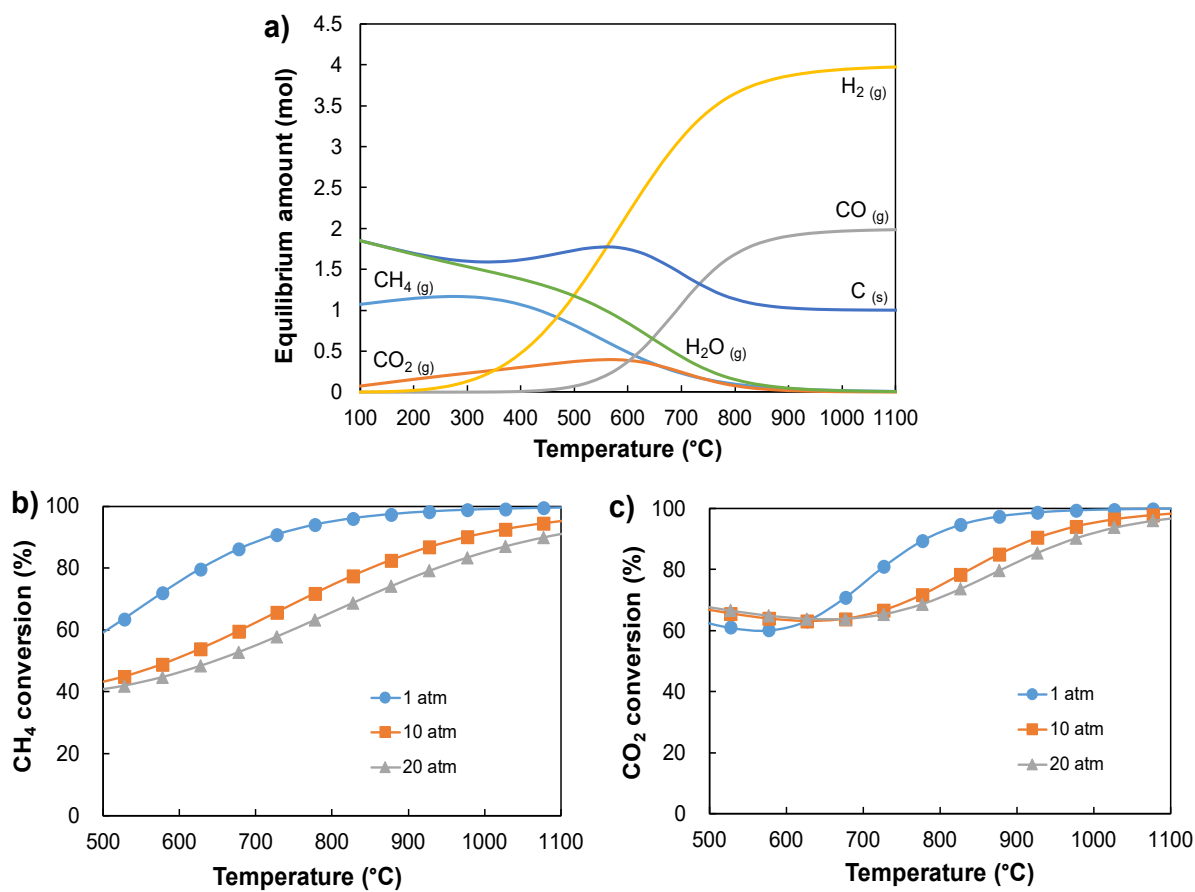


**Fig.S2 a)** Equilibrium products distribution for feed gases  $CH_4/CO_2 = 2$  at  $P = 1$  atm vs. temperature. Data were obtained from the FactSage. **b)** Equilibrium  $CH_4$  conversion versus temperature at 1 atm, 10 atm, and 20 atm reaction pressure. **c)** Equilibrium  $CO_2$  conversion versus temperature at 1 atm, 10 atm, and 20 atm reaction pressure.

## 5. Bubble column performance

A bubble column reactor provides a configuration to avoid catalyst deactivation via carbon deposition and has a higher surface area than the surface reactor reported above which allows us to achieve higher conversions. An experiment testing the catalyst stability while feeding 2:1 CH<sub>4</sub>:CO<sub>2</sub> on molten 20:80 mol% Sn-In catalyst was done in a bubble column reactor at 1016 °C over 22 hours (Fig.S3a). The CH<sub>4</sub> conversion remained at 20 ± 1%, and CO<sub>2</sub> the conversion gradually increased from 24.5% during the first 12 hours, before stabilizing at 30 ± 1%. Neither CH<sub>4</sub> nor CO<sub>2</sub> conversions decreased significant over 22 hours. The increasing CO<sub>2</sub> conversion observed during the first 12 hours may be because of carbon build-up on top of the melt, creating an avenue for CO<sub>2</sub> to react with C via the reverse Boudouard reaction ( $\text{CO}_2 + \text{C} \rightarrow 2 \text{CO}$ ). Another observation is that the CO<sub>2</sub> conversion is higher than CH<sub>4</sub> conversion in the bubble column reactor, which is different than the results from the surface reactor. The initial activity was measured in the surface reactor with a short reaction time, so carbon had little time to accumulate, which may have resulted in less reverse Boudouard reaction occurring in the surface reactor than in the bubble column. The conversion of reactants was also measured as a function of reaction temperature after the stability test. The maximum temperature tested was 1170 °C, at which 83.4% of CH<sub>4</sub> conversion and 93.3% CO<sub>2</sub> conversion were observed (Fig.S3b).

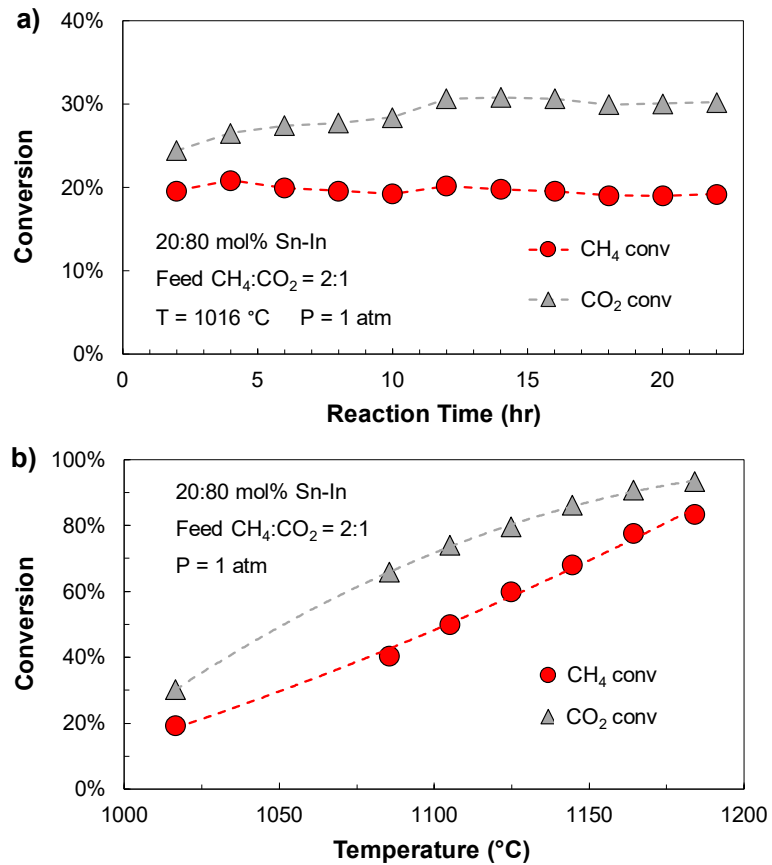


**Fig.S3 a)** CH<sub>4</sub> and CO<sub>2</sub> conversion of the combination of DRM and methane pyrolysis catalyzed by 20:80 mol% Sn:In molten metal inside bubble column reactor over 22 hours. The reaction temperature is 1000 °C and pressure is 1 atm inside the reactor. **b)** Reaction performance in a 20:80 mol% Sn:In molten alloy after the stability test in a). For both a) and b), a mixture of methane (2 sccm), CO<sub>2</sub> (1 sccm) and argon (3 sccm) were continuously introduced to the system at the level of 0.5 cm from the bottom and the melt height was ≈12cm.

## 6. Carbon characterization

### 6.1 Surface reactor

The crucible cup containing the metal was cooled after the reaction and characterized by the Hitachi S2600N Variable Pressure SEM at the UBC Bioimaging facility. Since the metal was difficult to remove without breaking the crucible cup, the cup itself was also placed in the SEM. Fig.S4a shows the fresh 50:50 mol% Sn-In without undergoing any reactions, while Fig.S4b depicts the exhausted 50:50 mol% Sn-In after 40 minutes of reaction. Despite the 40 minutes of reaction time, the surface was not completely covered by carbon. Therefore, choosing 20 minutes as the time on stream for comparing the activity of different alloys is reasonable due to the insignificant catalyst deactivation.

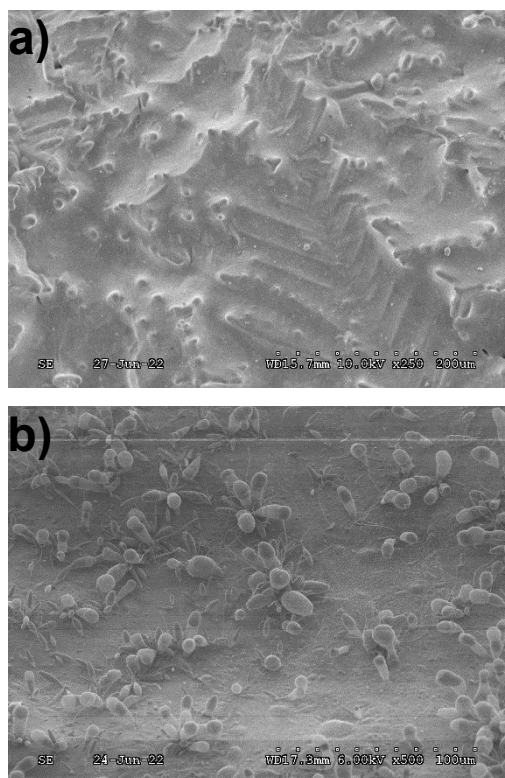


**Fig.S4 a)** SEM image of fresh 50:50 mol% Sn-In alloy after cooling. **b)** SEM image of 50:50 mol% Sn-In alloy surface over 40 mins reaction in the surface reactor. The reaction temperature is 980 °C, total pressure is 1 atm, total flow rate is 7 sccm, CH<sub>4</sub>:CO<sub>2</sub>:Ar = 2:1:4 mol, and the catalyst surface area is 0.50 cm<sup>2</sup>.

Carbon was removed from the surface of the 20:80 mol% Sn:In bubble column after 32 hours. This was done by allowing the metal alloy to cool to a solid and inverting the column to pour off the carbon. This carbon was analyzed by Zeiss CrossBeam350 CryoFIB SEM and EDX at UBC Bioimaging facility. Small metal particles, highlighted in the red square in Fig.S5a, were found on the carbon. Fig.S5b provides a zoomed-in picture of the metal particles shown in Fig.S5a. The metal particles are enriched in In, as indicated by the EDX results in Fig.S5c. Fig.S5d shows the combined elemental mapping for carbon samples, displaying the main elements C, In, O, and Sn. Fig.S5e-h display separate mappings for each element. The EDX mapping reveals that the metal particles formed spheres on the carbon. However, the carbon still exhibits high purity (>93%).

Fig.S6a shows a more zoomed-in picture of the metal particle. Two spots were chosen for EDX spot analysis (Fig.S6b): one on the spherical metal (spectrum 14) and one in the region next to the metal particle (spectrum 15). It is evident from the analysis that the metal particle is rich in In (Fig.S6c) with a ratio of 5:1 In to Sn (compared to 4:1 for the bulk catalyst), and the region adjacent to the metal particle consists of carbon with a purity exceeding 95 mol% (Fig.S6d). This indicates that the metals do not adhere to the carbon. Fig.S7 shows one metal particle on a different location, similar results were obtained, and 100% purity of carbon was found next to the metal particle. Thus, by employing proper heat treatment (to evaporate the metal) or acid treatment (to dissolve the metal), the metals can be removed from the carbon, resulting in higher purity carbon.

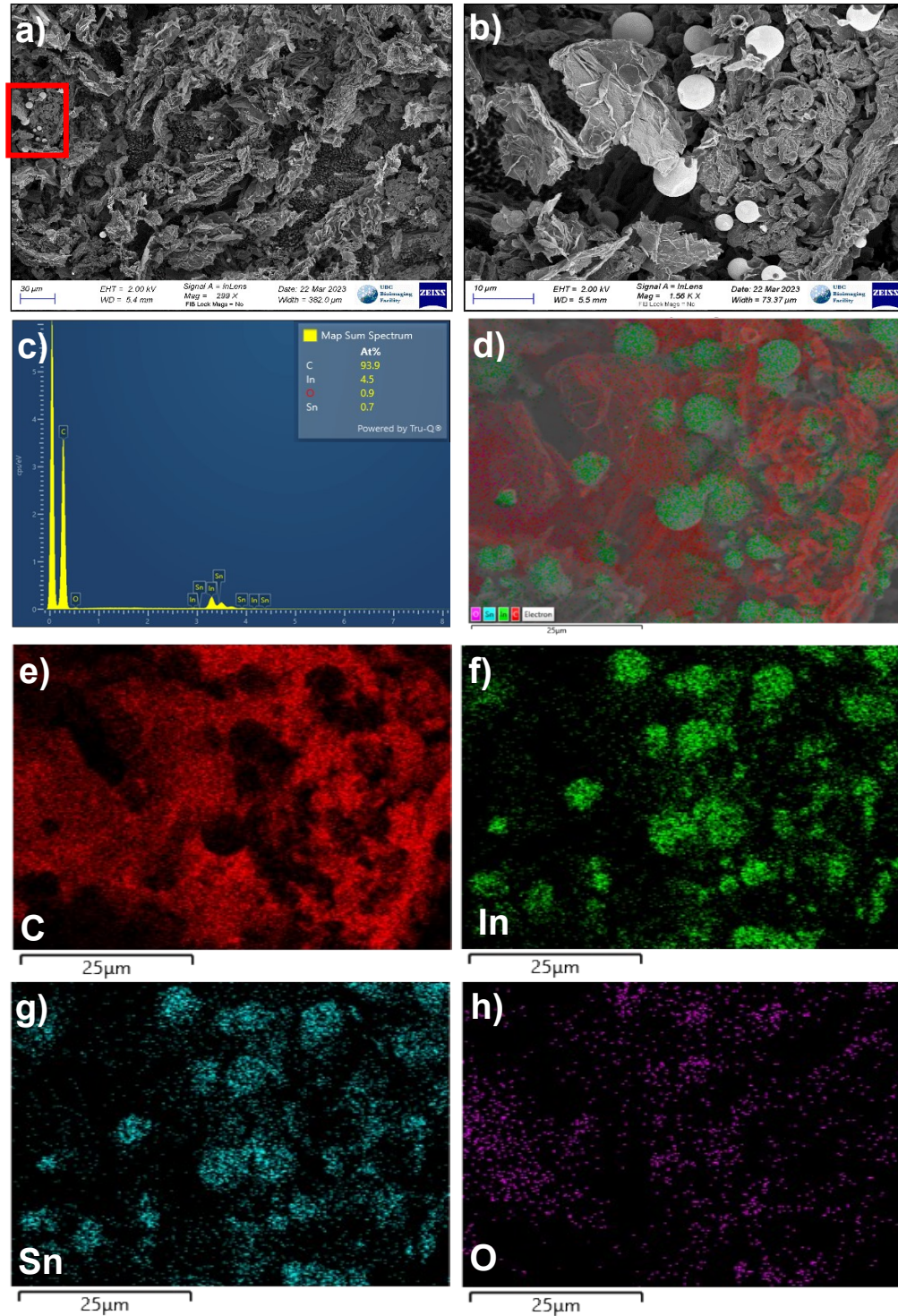


**Fig.S5 a)** SEM images of carbon collected from surface of the melt after cooling with metal particles shown in red square. **b)** SEM images of carbon with metal particles at higher magnification. **c)** EDX results for b). **d)** Overall EDX elemental mapping for element C, In, Sn and O. **e) - h)** EDX elemental mapping for element C (red), In (green), Sn (blue) and O (purple).

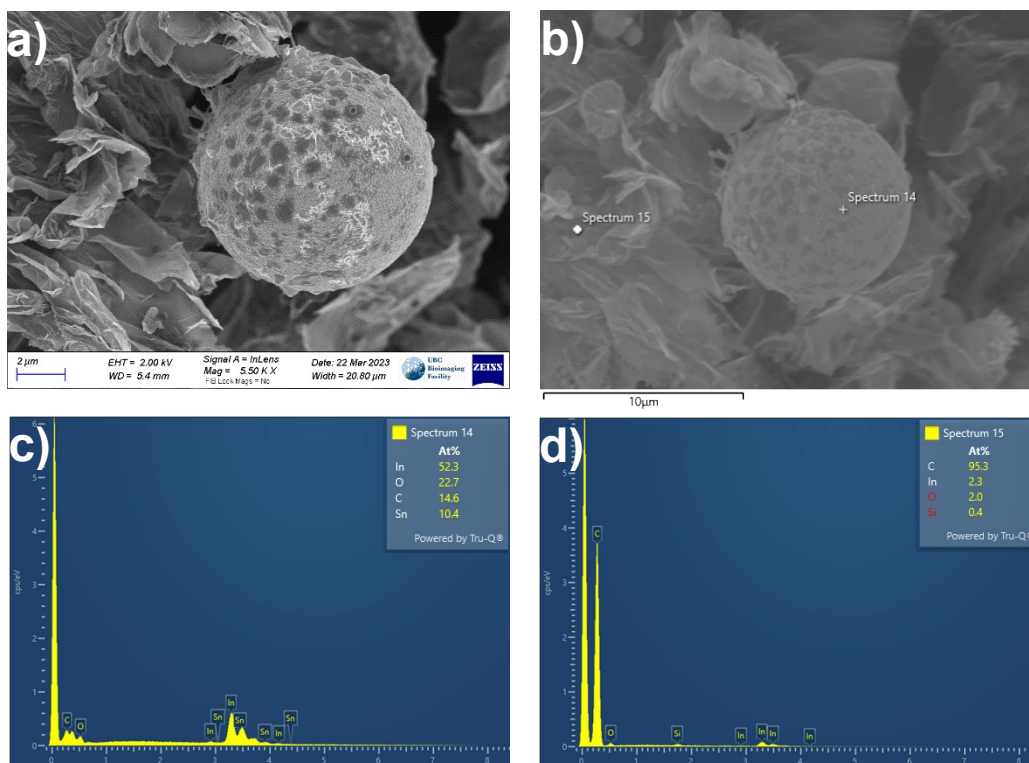


**Fig.S6 a)** SEM images of one metal particle on the carbon **b)** Two spots were chosen for EDX spot analysis: on the spherical metal (spectrum 14) and in region next to the metal particle (spectrum 15) **c)** EDX results for spherical metal (spectrum 14). **d)** EDX results for the region next to the metal particle (spectrum 15).

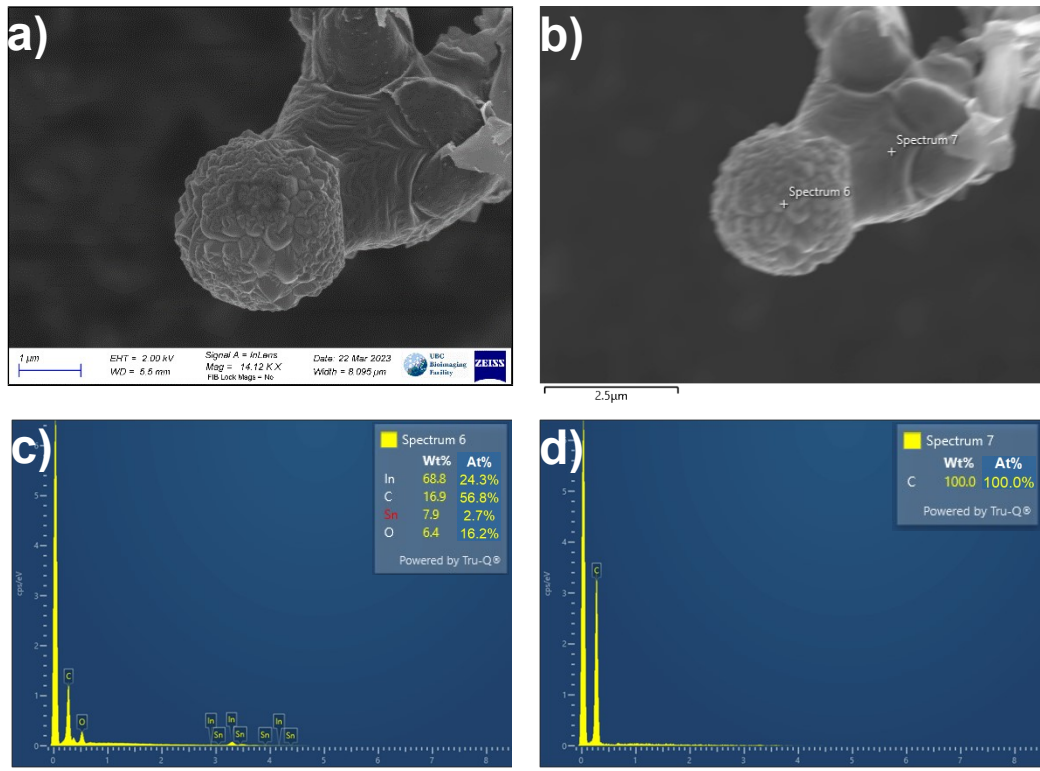


Fig.S7 a) SEM images of one metal particle on the carbon b) Two spots were chosen for EDX spot analysis: on the spherical metal (spectrum 6) and in region next to the metal particle (spectrum 7) c) EDX results for spherical metal (spectrum 6). d) EDX results for the region next to the metal particle (spectrum 7).

## 7. References

- 1 C. Palmer, D. C. Upham, S. Smart, M. J. Gordon, H. Metiu and E. W. McFarland, *Nat Catal*, 2020, **3**, 83–89.
- 2 Z. Zong, G. Cai, M. Tabbara and D. Chester Upham, *Energy Convers Manag*, 2023, **277**, 116624.
- 3 C. W. Bale, E. Bélisle, P. Chartrand, S. A. Deckerov, G. Eriksson, A. E. Gheribi, K. Hack, I. H. Jung, Y. B. Kang, J. Melançon, A. D. Pelton, S. Petersen, C. Robelin, J. Sangster, P. Spencer and M. A. Van Ende, *Calphad*, 2016, **54**, 35–53.